

## Supporting Information

### Atom-precise incorporation of platinum in ultrafine transition metal carbides for efficient synergistic electrochemical hydrogen evolution

Xingxing Pan,<sup>a</sup> Shuanglong Lu,\*<sup>a</sup> Duo Zhang,<sup>b</sup> Ye Zhang,<sup>c</sup> Fang Duan,<sup>a</sup> Han Zhu,<sup>a</sup> Hongwei Gu,<sup>d</sup> Shua Wang<sup>b</sup> and Mingliang Du\*<sup>a</sup>

### Contents

<b>Fig S1.</b> (a, b, c) SEM and (d, e, f) HR-TEM images of the as-synthesized Pt-CNFs, $\alpha$ -MoC <sub>1-x</sub> -CNFs and Pt/ $\alpha$ -MoC <sub>1-x</sub> -CNFs. ....	3
<b>Fig S2.</b> HR-TEM images of the as-synthesized Pt/ $\alpha$ -MoC <sub>1-x</sub> -CNFs with different molar ratios between Pt(acac) <sub>2</sub> and PMA: (a) Pt/ $\alpha$ -MoC <sub>1-x</sub> -CNFs-1, (b) Pt/ $\alpha$ -MoC <sub>1-x</sub> -CNFs-2, (c) Pt/ $\alpha$ -MoC <sub>1-x</sub> -CNFs-3 and (d) Pt/ $\alpha$ -MoC <sub>1-x</sub> -CNFs-4.....	3
<b>Fig S3.</b> XRD spectra of $\alpha$ -MoC <sub>1-x</sub> -CNFs, Pt/ $\alpha$ -MoC <sub>1-x</sub> -CNFs-1, Pt/ $\alpha$ -MoC <sub>1-x</sub> -CNFs-2, Pt/ $\alpha$ -MoC <sub>1-x</sub> -CNFs-3 and Pt/ $\alpha$ -MoC <sub>1-x</sub> -CNFs-4. ....	4
<b>Fig S4.</b> (a, b, c) SEM and (d, e, f) HR-TEM images of the as-synthesized Pt/ $\alpha$ -MoC <sub>1-x</sub> -CNFs-0.1, Pt/ $\alpha$ -MoC <sub>1-x</sub> -CNFs-0.2 and Pt/ $\alpha$ -MoC <sub>1-x</sub> -CNFs-0.3. ....	4
<b>Fig S5.</b> HR-TEM images of (a) Pt/ $\alpha$ -MoC <sub>1-x</sub> -CNFs-2-800, (b) Pt/ $\alpha$ -MoC <sub>1-x</sub> -CNFs-2-900, (c) Pt/ $\alpha$ -MoC <sub>1-x</sub> -CNFs-2-1000, (d) Pt/ $\alpha$ -MoC <sub>1-x</sub> -CNFs-2-1100 and (e) Pt/ $\alpha$ -MoC <sub>1-x</sub> -CNFs-2-1200. ....	5
<b>Fig S6.</b> XRD pattern of Pt/ $\alpha$ -MoC <sub>1-x</sub> -CNFs-2-800, Pt/ $\alpha$ -MoC <sub>1-x</sub> -CNFs-2-900, Pt/ $\alpha$ -MoC <sub>1-x</sub> -CNFs-2-1000, Pt/ $\alpha$ -MoC <sub>1-x</sub> -CNFs-2-1100 and Pt/ $\alpha$ -MoC <sub>1-x</sub> -CNFs-2-1200. ....	5
<b>Fig S7.</b> Raman spectra of the as-produced Pt/ $\alpha$ -MoC <sub>1-x</sub> -CNFs-2 obtained at different decomposition temperatures. ....	6
<b>Fig S8.</b> HER polarization curves of Pt/ $\alpha$ -MoC <sub>1-x</sub> -CNFs with different doped amounts of Pt in 0.5 M H <sub>2</sub> SO <sub>4</sub> solution. ....	6
<b>Fig S9.</b> (a-e) CV polarization curves of Pt/ $\alpha$ -MoC <sub>1-x</sub> -CNFs-1, Pt/ $\alpha$ -MoC <sub>1-x</sub> -CNFs-2, Pt/ $\alpha$ -MoC <sub>1-x</sub> -CNFs-3, Pt/ $\alpha$ -MoC <sub>1-x</sub> -CNFs-4 and Pt-CNFs in the nonfaradaic region with scan rates from 5 to 200 mV s <sup>-1</sup> . (f) The double-layer capacitance (C <sub>dl</sub> ) of Pt/ $\alpha$ -MoC <sub>1-x</sub> -CNFs-1, Pt/ $\alpha$ -MoC <sub>1-x</sub> -CNFs-2, Pt/ $\alpha$ -MoC <sub>1-x</sub> -CNFs-3, Pt/ $\alpha$ -MoC <sub>1-x</sub> -CNFs-4 and Pt-CNFs. ....	7
<b>Fig S10.</b> (a) HER polarization curves of Pt/ $\alpha$ -MoC <sub>1-x</sub> -CNFs-2 obtained under different pyrolysis temperature and Pt/C in 0.5 M H <sub>2</sub> SO <sub>4</sub> solution. (b) Corresponding Tafel slopes derived from (a). ....	7
<b>Fig S11.</b> EIS Nyquist plots of Pt/ $\alpha$ -MoC <sub>1-x</sub> -CNFs-1, Pt/ $\alpha$ -MoC <sub>1-x</sub> -CNFs-2, Pt/ $\alpha$ -MoC <sub>1-x</sub> -	

CNFs-3 and Pt/ $\alpha$ -MoC <sub>1-x</sub> -CNFs-4 .....	8
<b>Fig S12.</b> SEM images of the Pt/ $\alpha$ -MoC <sub>1-x</sub> -CNFs-2 catalyst before (a) and after (c) HER. HR-TEM images of the Pt/ $\alpha$ -MoC <sub>1-x</sub> -CNFs-2 catalyst before (b) and after (d) HER .....	8
<b>Fig S13.</b> (a) SEM and (b) HR-TEM images of the as-synthesized Pt/(Fe-C <sub>x</sub> )-CNFs; (c) SEM and (d) HR-TEM images of Ni/(W-C <sub>x</sub> )-CNFs.....	9
<b>Fig S14.</b> HR-TEM image of WC <sub>x</sub> NPs in Pt/WC <sub>x</sub> -CNFs. ....	9
<b>Fig S15.</b> HR-TEM images of (a) Pt/WC <sub>x</sub> -CNFs and (b) WC <sub>x</sub> -CNFs.....	10
<b>Fig S16.</b> HAADF-STEM-EDS elemental mapping images of Pt/WC <sub>x</sub> -CNFs. ....	10
<b>Fig S17.</b> XRD pattern of the Pt/WC <sub>x</sub> -CNFs and WC <sub>x</sub> -CNFs.....	11
<b>Fig S18.</b> (a) EIS Nyquist plots of WC <sub>x</sub> -CNFs and Pt/WC <sub>x</sub> -CNFs-3 catalysts, the inset plot is the local enlarged view of the EIS. (b) Stability test of Pt/WC <sub>x</sub> -CNFs-3 through potential cycling, before and after 5000 cycles. ....	11
<b>Table S1.</b> Summary of all samples in the paper and their HER performance in 0.5 M H <sub>2</sub> SO <sub>4</sub> solution.....	11
<b>Table S2.</b> Comparison of the HER performance for Pt/TMCs-CNFs catalyst with other Pt-based, Mo-based or other transition metal carbide electrocatalysts in 0.5 M H <sub>2</sub> SO <sub>4</sub> solution. ....	12
<b>Supplementary References.....</b>	13

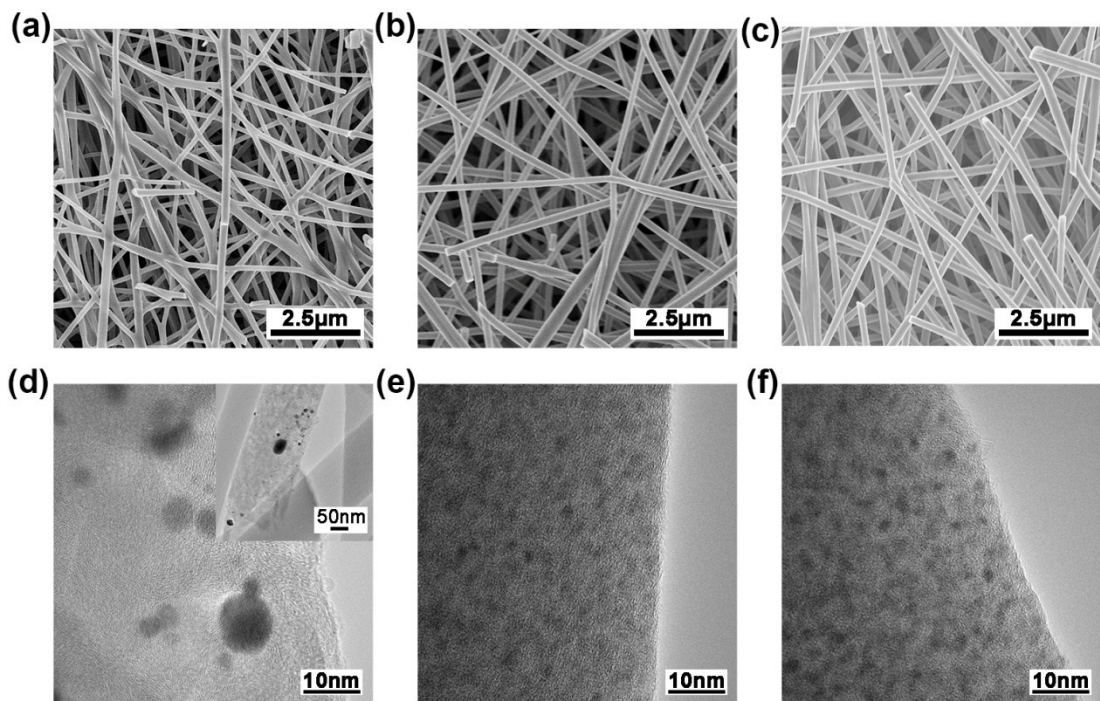


**Fig S1.** (a, b, c) SEM and (d, e, f) HR-TEM images of the as-synthesized Pt-CNFs,  $\alpha$ -MoC<sub>1-x</sub>-CNFs and Pt/ $\alpha$ -MoC<sub>1-x</sub>-CNFs.

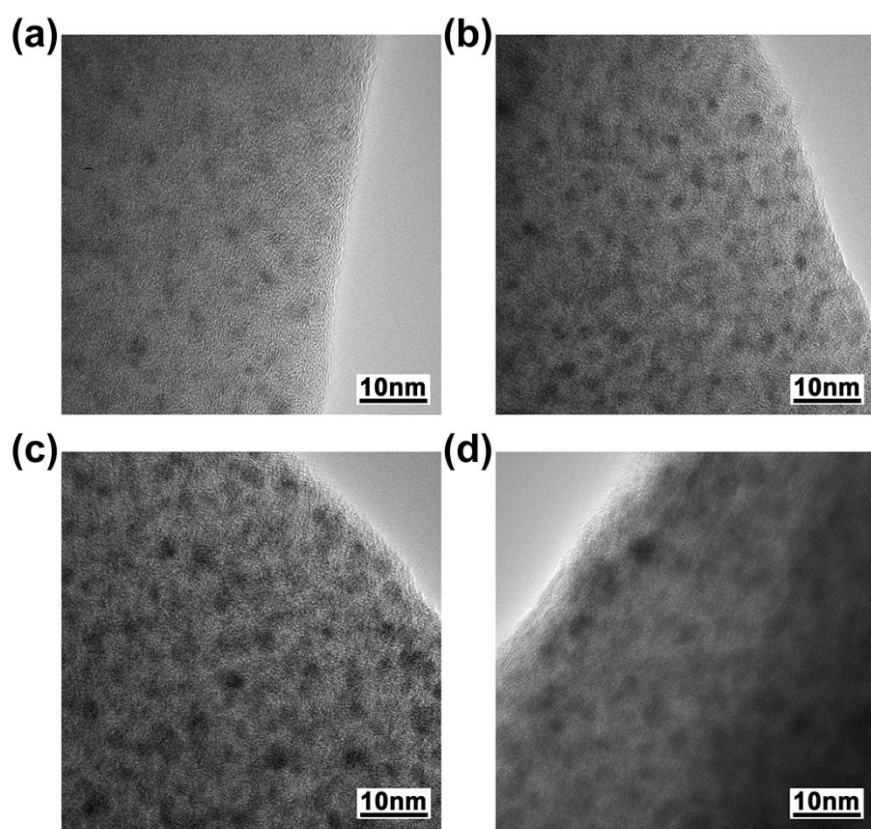


**Fig S2.** HR-TEM images of the as-synthesized Pt/ $\alpha$ -MoC<sub>1-x</sub>-CNFs with different molar ratios between Pt(acac)<sub>2</sub> and PMA: (a) Pt/ $\alpha$ -MoC<sub>1-x</sub>-CNFs-1, (b) Pt/ $\alpha$ -MoC<sub>1-x</sub>-CNFs-2, (c) Pt/ $\alpha$ -MoC<sub>1-x</sub>-CNFs-3 and (d) Pt/ $\alpha$ -MoC<sub>1-x</sub>-CNFs-4.

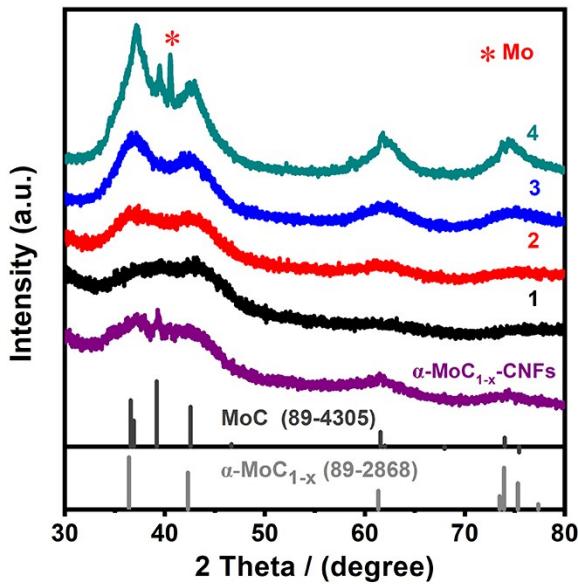


**Fig S3.** XRD spectra of  $\alpha\text{-MoC}_{1-x}\text{-CNFs}$ , Pt/ $\alpha\text{-MoC}_{1-x}\text{-CNFs}$ -1, Pt/ $\alpha\text{-MoC}_{1-x}\text{-CNFs}$ -2, Pt/ $\alpha\text{-MoC}_{1-x}\text{-CNFs}$ -3 and Pt/ $\alpha\text{-MoC}_{1-x}\text{-CNFs}$ -4.

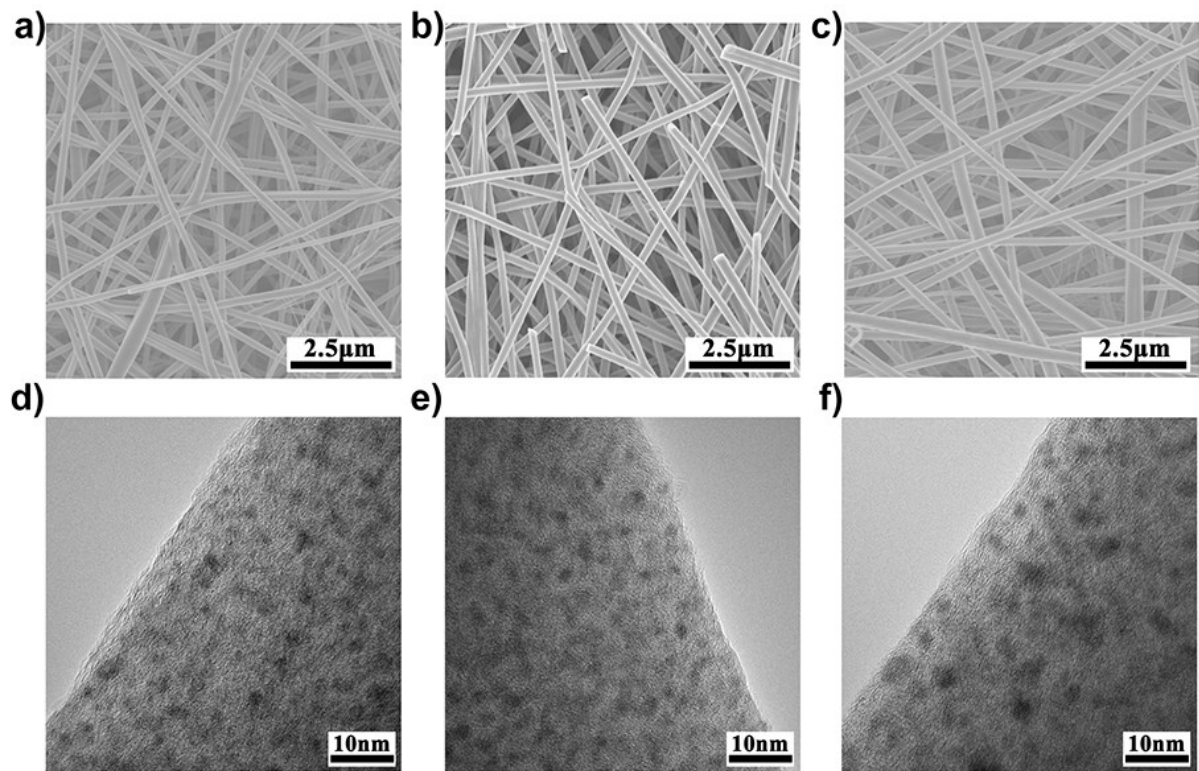


**Fig S4.** (a, b, c) SEM and (d, e, f) HR-TEM images of the as-synthesized Pt/ $\alpha\text{-MoC}_{1-x}\text{-CNFs}$ -0.1, Pt/ $\alpha\text{-MoC}_{1-x}\text{-CNFs}$ -0.2 and Pt/ $\alpha\text{-MoC}_{1-x}\text{-CNFs}$ -0.3.

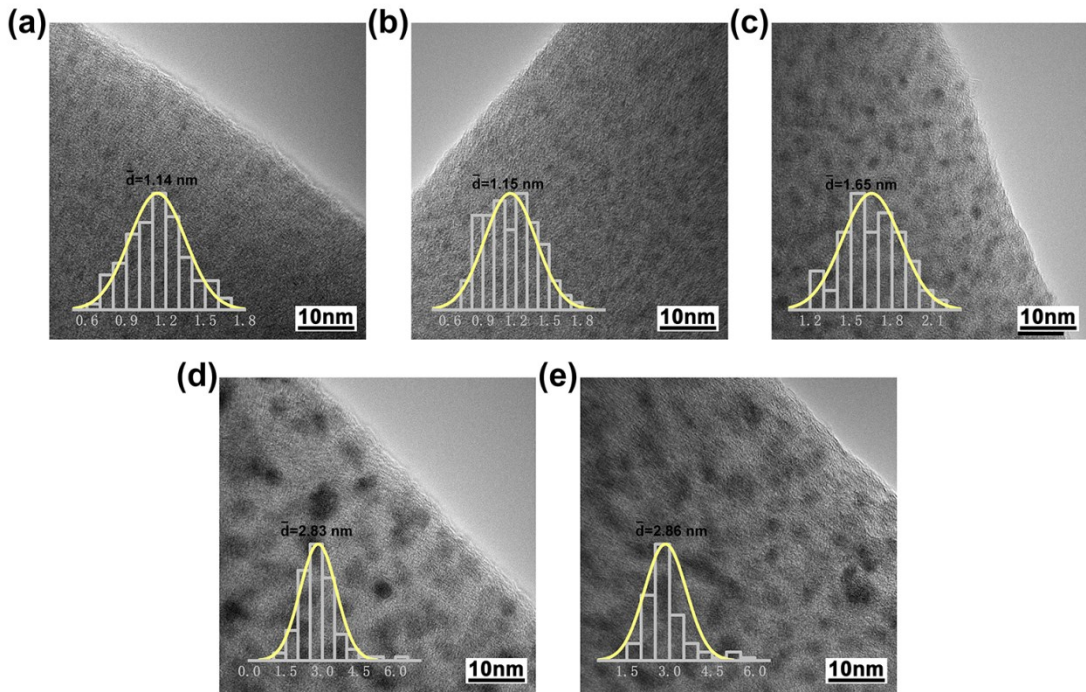


**Fig S5.** HR-TEM images of (a) Pt/ $\alpha$ -MoC<sub>1-x</sub>-CNFs-2-800, (b) Pt/ $\alpha$ -MoC<sub>1-x</sub>-CNFs-2-900, (c) Pt/ $\alpha$ -MoC<sub>1-x</sub>-CNFs-2-1000, (d) Pt/ $\alpha$ -MoC<sub>1-x</sub>-CNFs-2-1100 and (e) Pt/ $\alpha$ -MoC<sub>1-x</sub>-CNFs-2-1200.

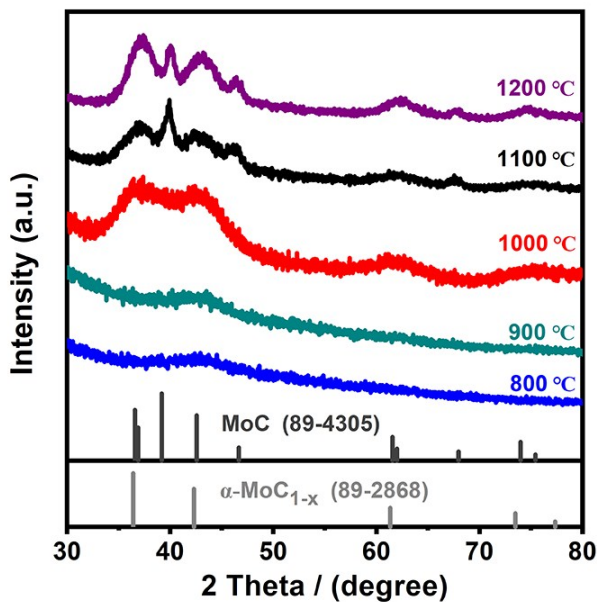


**Fig S6.** XRD pattern of Pt/ $\alpha$ -MoC<sub>1-x</sub>-CNFs-2-800, Pt/ $\alpha$ -MoC<sub>1-x</sub>-CNFs-2-900, Pt/ $\alpha$ -MoC<sub>1-x</sub>-CNFs-2-1000, Pt/ $\alpha$ -MoC<sub>1-x</sub>-CNFs-2-1100 and Pt/ $\alpha$ -MoC<sub>1-x</sub>-CNFs-2-1200.

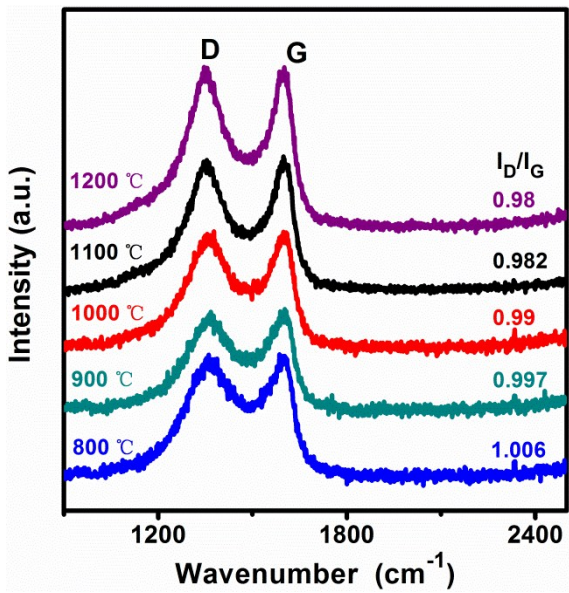


**Fig S7.** Raman spectra of the as-produced  $\text{Pt}/\alpha\text{-MoC}_{1-x}\text{-CNFs-2}$  obtained at different decomposition temperatures.

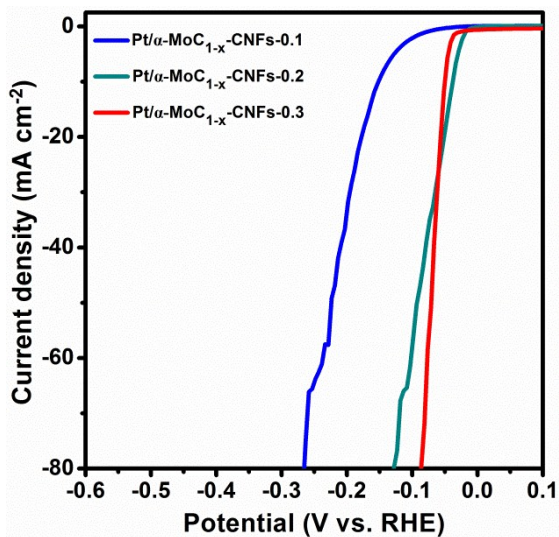


**Fig S8.** HER polarization curves of  $\text{Pt}/\alpha\text{-MoC}_{1-x}\text{-CNFs}$  with different doped amounts of Pt in 0.5 M  $\text{H}_2\text{SO}_4$  solution.

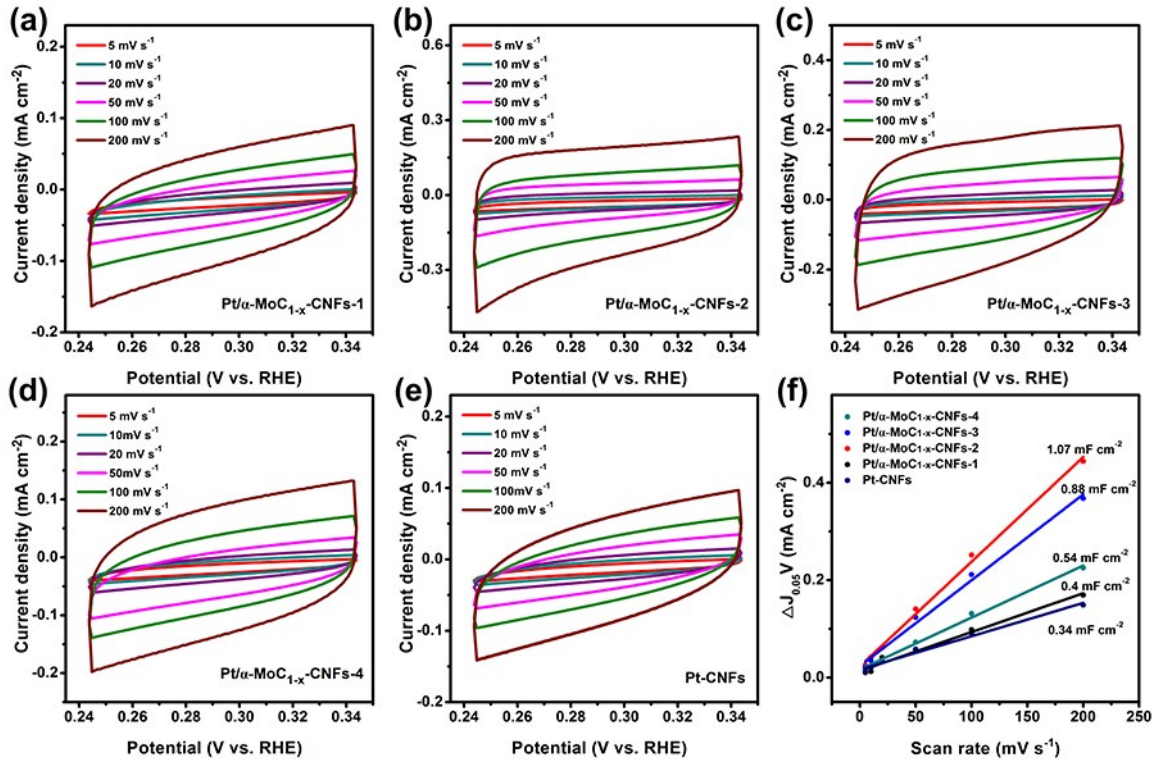


**Fig S9.** (a-e) CV polarization curves of Pt/ $\alpha$ -MoC<sub>1-x</sub>-CNFs-1, Pt/ $\alpha$ -MoC<sub>1-x</sub>-CNFs-2, Pt/ $\alpha$ -MoC<sub>1-x</sub>-CNFs-3, Pt/ $\alpha$ -MoC<sub>1-x</sub>-CNFs-4 and Pt-CNFs in the nonfaradaic region with scan rates from 5 to 200 mV s<sup>-1</sup>. (f) The double-layer capacitance ( $C_{dl}$ ) of Pt/ $\alpha$ -MoC<sub>1-x</sub>-CNFs-1, Pt/ $\alpha$ -MoC<sub>1-x</sub>-CNFs-2, Pt/ $\alpha$ -MoC<sub>1-x</sub>-CNFs-3, Pt/ $\alpha$ -MoC<sub>1-x</sub>-CNFs-4 and Pt-CNFs.

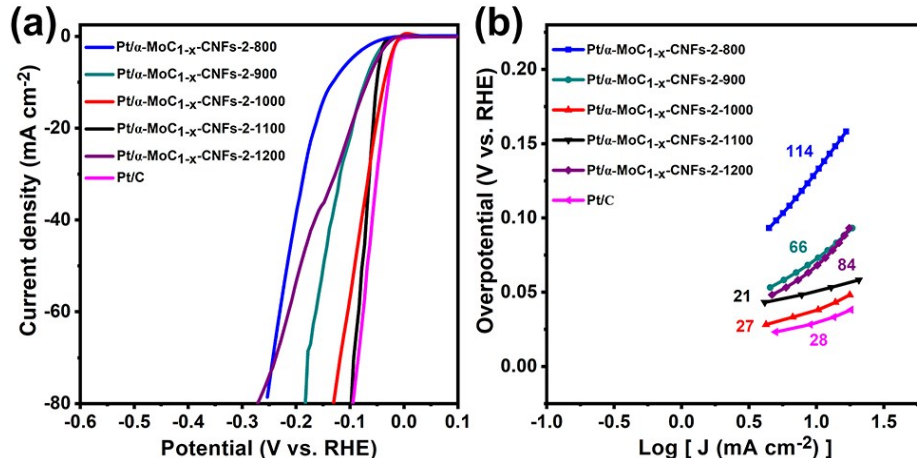


**Fig S10.** (a) HER polarization curves of Pt/ $\alpha$ -MoC<sub>1-x</sub>-CNFs-2 obtained under different pyrolysis temperature and Pt/C in 0.5 M H<sub>2</sub>SO<sub>4</sub> solution. (b) Corresponding Tafel slopes derived from (a).

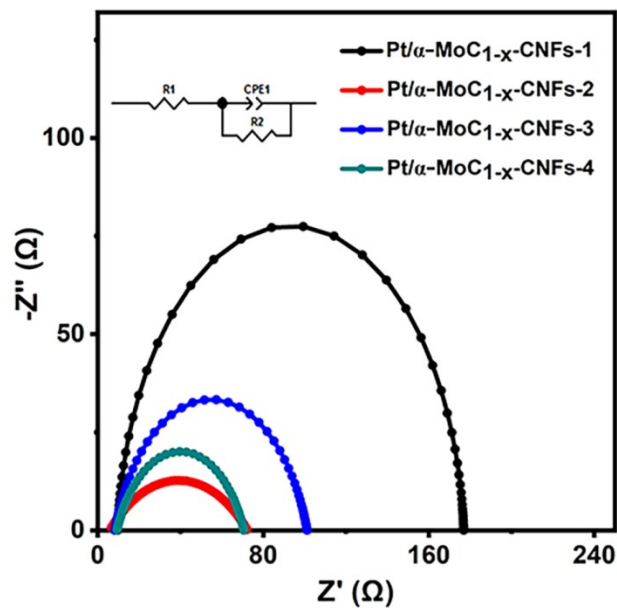


**Fig S11.** EIS Nyquist plots of Pt/ $\alpha$ -MoC<sub>1-x</sub>-CNFs-1, Pt/ $\alpha$ -MoC<sub>1-x</sub>-CNFs-2, Pt/ $\alpha$ -MoC<sub>1-x</sub>-CNFs-3 and Pt/ $\alpha$ -MoC<sub>1-x</sub>-CNFs-4.

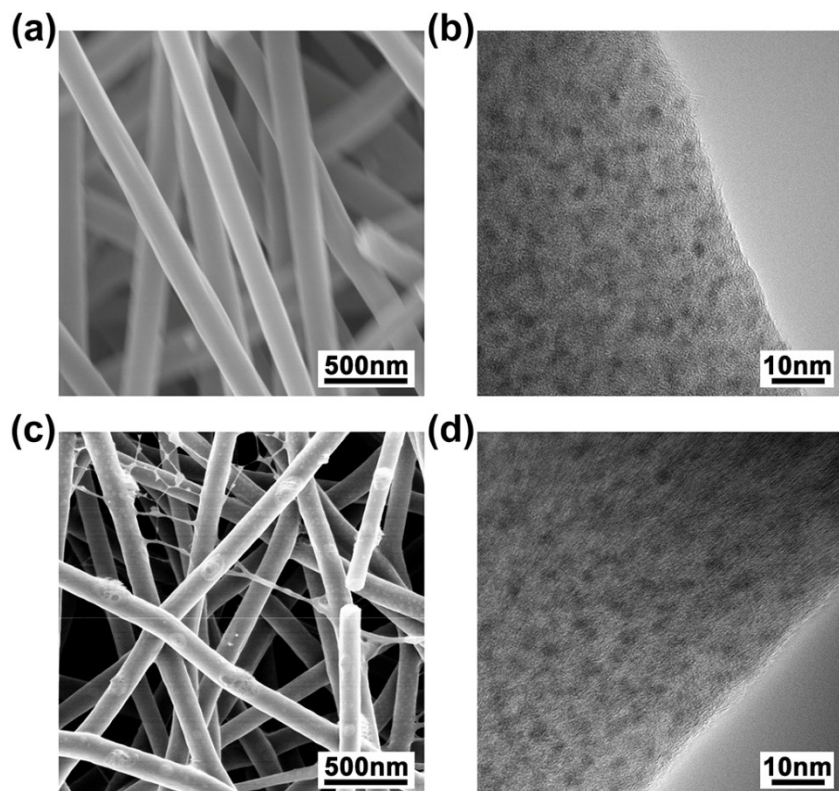


**Fig S12.** SEM images of the Pt/ $\alpha$ -MoC<sub>1-x</sub>-CNFs-2 catalyst before (a) and after (c) HER. HR-TEM images of the Pt/ $\alpha$ -MoC<sub>1-x</sub>-CNFs-2 catalyst before (b) and after (d) HER.

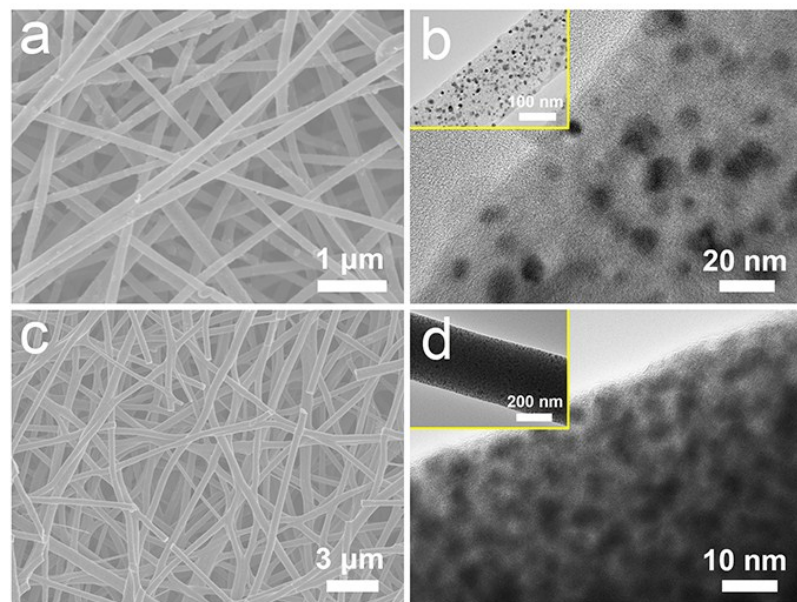


**Fig S13.** (a) SEM and (b) HR-TEM images of the as-synthesized Pt/(Fe-C<sub>x</sub>)-CNFs ; (c) SEM and (d) HR-TEM images of Ni/(W-C<sub>x</sub>)-CNFs.

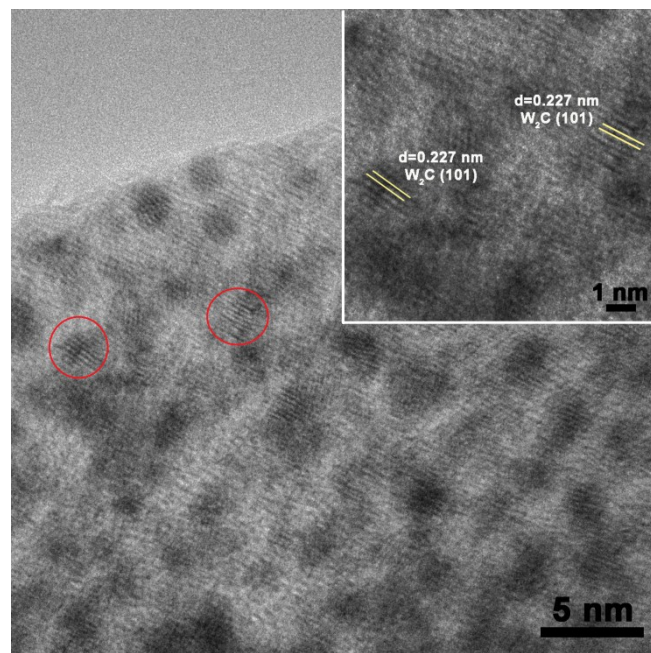


**Fig S14.** HR-TEM image of WC<sub>x</sub> NPs in Pt/WC<sub>x</sub>-CNFs.

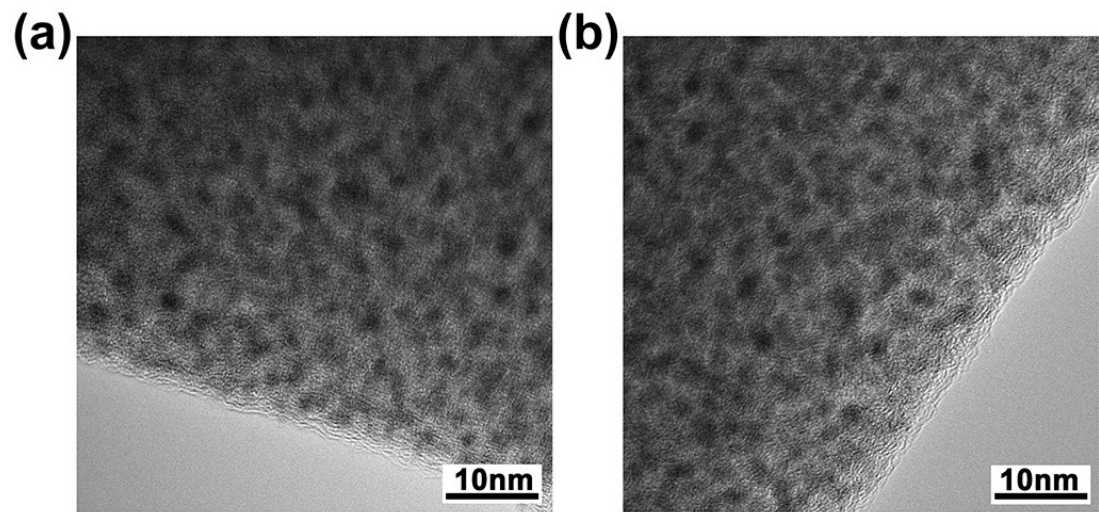


**Fig S15.** HR-TEM images of (a) Pt/WC<sub>x</sub>-CNFs and (b) WC<sub>x</sub>-CNFs.

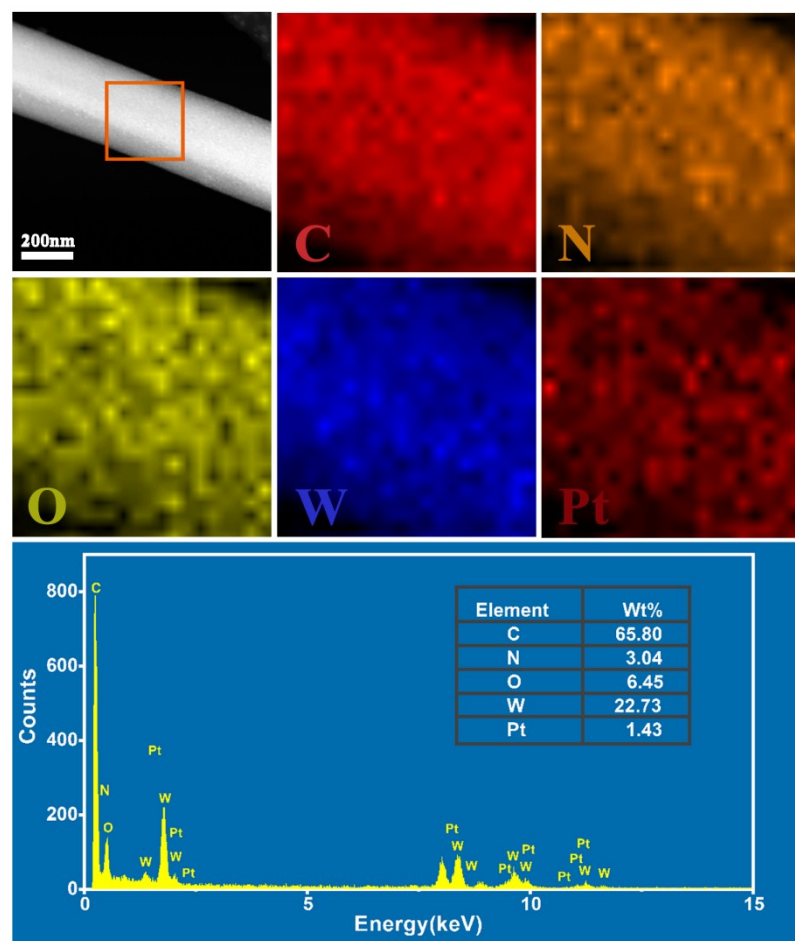


**Fig S16.** HAADF-STEM-EDS elemental mapping images of Pt/WC<sub>x</sub>-CNFs.

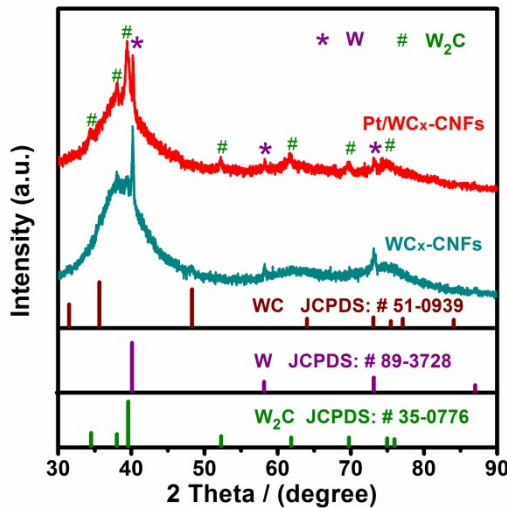


**Fig S17.** XRD pattern of the Pt/WCx-CNFs and WCx-CNFs.

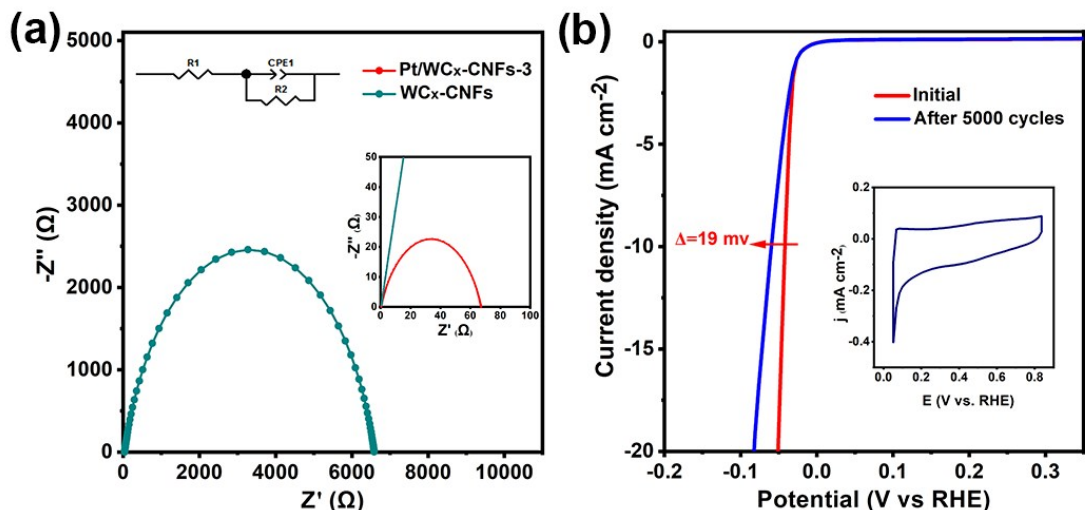


**Fig S18.** (a) EIS Nyquist plots of WC<sub>x</sub>-CNFs and Pt/WC<sub>x</sub>-CNFs-3 catalysts, the inset plot is the local enlarged view of the EIS. (b) Stability test of Pt/WC<sub>x</sub>-CNFs-3 through potential cycling, before and after 5000 cycles.

**Table S1.** Summary of all samples in the paper and their HER performance in 0.5 M H<sub>2</sub>SO<sub>4</sub> solution.

Catalyst	Molar Feeding Ratios of Pt(acac) <sub>2</sub> / HPA (mmol) (Final Pt content if it is available)	$\eta_{10}$ (mV)	Tafel slope (mV dec <sup>-1</sup> )
Pt/ $\alpha$ -MoC <sub>1-x</sub> -CNFs-1	same amount of Pt(acac) <sub>2</sub> used	0.2 / 0.05	104
Pt/ $\alpha$ -MoC <sub>1-x</sub> -CNFs-2		0.2 / 0.1 (1.5 wt% Pt)	38
Pt/ $\alpha$ -MoC <sub>1-x</sub> -CNFs-3		0.2 / 0.15	59
Pt/ $\alpha$ -MoC <sub>1-x</sub> -CNFs-4		0.2 / 0.2	73
Pt-CNFs		0.2 / ---	348
$\alpha$ -MoC <sub>1-x</sub> -CNFs	--- / 0.1	318	133
Pt/ $\alpha$ -MoC <sub>1-x</sub> -CNFs-0.1	0.1 / 0.1	152	81
Pt/ $\alpha$ -MoC <sub>1-x</sub> -CNFs-0.3	0.3 / 0.1 (3.3 wt% Pt)	50	20
Pt/ $\alpha$ -MoC <sub>1-x</sub> -CNFs-800	0.2 / 0.1	133	114
Pt/ $\alpha$ -MoC <sub>1-x</sub> -CNFs-900	0.2 / 0.1	73	66
Pt/ $\alpha$ -MoC <sub>1-x</sub> -CNFs-1100	0.2 / 0.1	50	21

Pt/ $\alpha$ -MoC <sub>1-x</sub> -CNFs-1200		0.2 / 0.1	68	84
Pt/WC <sub>x</sub> -CNFs-1	same amount of Pt(acac) <sub>2</sub> used	0.2 / 0.05	47	44
Pt/WC <sub>x</sub> -CNFs-2		0.2 / 0.1	51	50
Pt/WC <sub>x</sub> -CNFs-3		0.2 / 0.15 (2.4 wt% Pt)	42	25
WC <sub>x</sub> -CNFs	--- / 0.15		>500	274
Pt/C	(20 wt% Pt)		30	28

**Table S2.** Comparison of the HER performance for Pt/TMCs-CNFs catalyst with other Pt-based, Mo-based or other transition metal carbide electrocatalysts in 0.5 M H<sub>2</sub>SO<sub>4</sub> solution.

Catalyst	content of Pt (wt%)	$\eta_{10}$ (mV)	Tafel slope (mV dec <sup>-1</sup> )	Journal	Reference
Pt/ $\alpha$ -MoC <sub>1-x</sub> -CNFs-2	1.5	38	27	This work	
Pt/WC <sub>x</sub> -CNFs-3	2.4	42	25	This work	
Pt@Fe-N-C	2.1	60	42	Advanced Energy Material, 2017	[1]
Mo <sub>2</sub> TiC <sub>2</sub> T <sub>x</sub> -Pt <sub>SA</sub>	1.2	30	30	Nature Catalysis, 2018	[2]
ALD Pt/N-GO	2.1	38	29	Nature Communication, 2016	[3]
Pt@PCM	0.53	105	65.3	Science Advances, 2018	[4]
MoC <sub>1-x</sub> /Pt NPs-600	3.0	30	31	Advanced Science, 2019	[5]
$\alpha$ -MoC <sub>1-x</sub> /NC		142	74	Sustainable Chemistry & Engineering, 2019	[6]
Mo- $\alpha$ -MoC <sub>1-x</sub>		115		Advanced Materials Interfaces, 2018	[7]
MoC@graphite		124	43	Journal of Materials Chemistry A, 2016	[8]
Mo <sub>2</sub> C/NCF		144	55	ACS Nano, 2016	[9]
MoC-Mo <sub>2</sub> C		126	43	Chemical Science, 2016	[10]
Ni-Mo <sub>2</sub> C		155	79	Chemical Communications, 2013	[11]
Co-Mo <sub>2</sub> C		140	39	Advanced Functional Materials, 2016	[12]
Mo <sub>2</sub> C-Co		48	39	Advanced Materials, 2018	[13]
Ni-WC		53	43.5	Energy & Environmental Science, 2018	[14]

WN <sub>x</sub> -NRPGC		132	86	Advanced Science, 2018	[15]
Mo <sub>2</sub> C@3DNMC		155	73	Electrochimica Acta	[16]
G@N-MoS <sub>2</sub>		243	82.5	Advanced Materials, 2018	[17]
h-MoN@BNCNT		78	46	Advanced Functional Materials, 2018	[18]

## Supplementary References

- 1 X. Zeng, J. Shui, X. Liu, Q. Liu, Y. Li, J. Shang, L. Zheng and R. Yu, *Adv. Energy Mater.*, 2018, **8**, 1701345.
- 2 J. Zhang, Y. Zhao, X. Guo, C. Chen, C. L. Dong, R. S. Liu, C. P. Han, Y. Li, Y. Gogotsi and G. Wang, *Nat. Catal.*, 2018, **1**, 985-992.
- 3 N. Cheng, S. Stambula, D. Wang, M. N. Banis, J. Liu, A. Riese, B. Xiao, R. Li, T. K. Sham, L. M. Liu, G. A. Botton and X. Sun, *Nat. Commun.*, 2016, **7**, 13638.
- 4 H. Zhang, P. An, W. Zhou, B. Y. Guan, P. Zhang, J. Dong and X. W. Lou, *Sci. Adv.*, 2018, **4**, 6657.
- 5 H. J. Song, M. C. Sung, H. Yoon, B. Ju and D. W. Kim, *Adv. Sci.*, 2019, **6**, 1802135.
- 6 L. Lin, Z. Sun, M. Yuan, H. Yang, H. Li, C. Nan, H. Jiang, S. Ge and G. Sun, *ACS Sustainable Chem. Eng.*, 2019, **7**, 9637-9645.
- 7 J. Diao, W. Yuan, Y. Su, Y. Qiu and X. Guo, *Adv. Mater. Interfaces*, 2018, **5**, 1800223.
- 8 Z. Shi, Y. Wang, H. Lin, H. Zhang, M. Shen, S. Xie, Y. Zhang, Q. Gao and Y. Tang, *J. Mater. Chem. A*, 2016, **4**, 6006-6013.
- 9 Y. Huang, Q. Gong, X. Song, K. Feng, K. Nie, F. Zhao, Y. Wang, M. Zeng, J. Zhong and Y. Li, *ACS Nano*, 2016, **10**, 11337-11343.
- 10 H. Lin, Z. Shi, S. He, X. Yu, S. Wang, Q. Gao and Y. Tang, *Chem. Sci.*, 2016, **7**, 3399-3405.
- 11 T. Ouyang, A. N. Chen, Z. Z. He, Z. Q. Liu and Y. Tong, *Chem. Commun.*, 2018, **54**, 9901-9904.
- 12 H. Lin, N. Liu, Z. Shi, Y. Guo, Y. Tang and Q. Gao, *Adv. Funct. Mater.*, 2016, **26**, 5590-5598.
- 13 X. Zang, W. Chen, X. Zou, J. N. Hohman, L. Yang, B. Li, M. Wei, C. Zhu, J. Liang, M. Sanghadasa, J. Gu and L. Lin, *Adv. Mater.*, 2018, **30**, 1805188.
- 14 Y. Y. Ma, Z. L. Lang, L. K. Yan, Y. H. Wang, H. Q. Tan, K. Feng, Y. J. Xia, J. Zhong,

- Y. Liu, Z. H. Kang and Y. G. Li, *Energy Environ. Sci.*, 2018, **11**, 2114-2123.
- 15 Y. Zhu, G. Chen, Y. Zhong, W. Zhou and Z. Shao, *Adv. Sci.*, 2018, **5**, 1700603.
- 16 K. An and X. Xu, *Electrochim. Acta*, 2019, **293**, 348-355.
- 17 C. Tang, L. Zhong, B. Zhang, H. F. Wang and Q. Zhang, *Adv. Mater.*, 2018, **30**, 1705110.
- 18 J. Miao, Z. Lang, X. Zhang, W. Kong, O. Peng, Y. Yang, S. Wang, J. Cheng, T. He, A. Amini, Q. Wu, Z. Zheng, Z. Tang and C. Cheng, *Adv. Funct. Mater.*, 2019, **29**, 1805893.